Functionalization of polypropylene via melt mixing

R. M. Ho, A. C. Su* and C. H. Wu
Institute of Materials Science and Engineering, National Sun Yat-Sen University, Kaohsiung, Taiwan 80424, ROC

and S. I. Chen
New Materials Research and Development, China Steel Corporation, Kaohsiung, Taiwan 81233, ROC

(Received 26 August 1992; revised 9 November 1992)

Grafting of maleic anhydride (MAH) onto isotactic polypropylene (PP) was performed by melt mixing in a laboratory-scale internal mixer with the addition of dicumyl peroxide (DCP) as an initiator. The efficiency of the graft reaction (estimated by use of Fourier-transform infra-red spectroscopy) tends to decrease with increasing MAH or DCP content; the optimal composition for the present reaction system appeared to be at a low DCP level and a moderate MAH loading. Concurrent with the grafting reaction, PP undergoes significant chain scission as indicated by the decrease in mixing torque and supported by the dynamic rheological evidence. The first addition of MAH to the reaction mixture enhanced the DCP-initiated chain scission; upon further addition of MAH, the scission reaction became less severe. These observations were explained in terms of competition between chain transfer/β scission and bimolecular coupling of radical intermediates.

(Keywords: polypropylene; functionalization; melt mixing; grafting; dynamic rheology; Fourier-transform infra-red spectroscopy)

INTRODUCTION

The modification of polyolefins by means of graft reactions, where a peroxide initiator (such as dicumyl peroxide, DCP) is used with an unsaturated functional monomer (such as maleic anhydride, MAH), has received much attention in the past several decades. Modification of polyolefins has been successfully achieved using solution, melt and even solid-state routes. The functionalized polymers have been extensively used for the compatibilization of immiscible polymer blends as well as the improvement of interfacial adhesion in polymeric composites[1,2]. In spite of the commercial success of functionalized polyolefins, the exact nature of the chemical paths involved in the functionalization process is not completely clear. It is generally agreed that, for the peroxide-initiated functionalization of polyolefins, crosslinking or chain scission may occur simultaneously with the graft reaction. For polyethylene (PE), the dominant side reaction is crosslinking[3]; for isotactic polypropylene (PP), the dominant side reaction is chain scission[4]. In the case of ethylene–propylene rubber (EPR), both crosslinking and chain scission may be important[5–8]. More detailed features of the functionalization process as well as structural characteristics of the functionalized product, however, appear to be different according to different researchers.

A typical example may be the graft reaction of MAH to PP. In an earlier study using a solution process, Minoura *et al.*[9] proposed that the graft reaction involves mainly the appending of MAH to tertiary carbons along the PP backbone; the possibility of MAH grafting to the end of degraded PP chains was also suggested. In a later study using a melt process, Gaylord and Mishra[4] suggested that MAH may be appended to tertiary sites along the PP backbone as single units or as short blocks, the latter being attributed to the homopolymerization of MAH. The notion of MAH homopolymerization during melt processing, however, has been ruled out as unlikely by Russell and Kelusky[10] based on ceiling temperature considerations. More recently, the ^{13}C n.m.r. analysis of Rengarajan *et al.*[11] indicated that the grafted MAH moieties may also form crosslinks between PP chains. Constable and Adur[12] indicated that their MAH-modified PP consists of a single anhydride ring grafted to the PP chain end.

Another controversial issue in the anhydride modification of PP is the effect of MAH on the extent of chain scission. It is generally agreed that, as a result of peroxide-initiated scission reactions, PP degrades extensively during the functionalization process[4,9]. The presence of MAH often alleviates the scission reactions[13]; this is expected since the simultaneous presence of an unsaturated species and a peroxide has been known[14,15] to enhance crosslinking of PP. Interestingly, Gaylord and Mishra[4] reported that the presence of MAH actually enhanced chain scission in their melt functionalization process. This observation, however, was not confirmed in later studies[13,16].

Reported here are results of our study on the grafting of MAH onto PP using a laboratory-scale internal mixer

---

*To whom correspondence should be addressed

0032-3861/93/153264–06

as the reactor where the mixing torque may be continuously monitored. The extent of grafting in the functionalized PP was estimated by use of Fourier-transform infra-red spectroscopy (*FT*i.r.). The extent of chain scission was monitored by means of dynamic rheological measurements.

EXPERIMENTAL

Materials

A commercial PP sample with a melt flow index of 1.8 dg min^{-1} (at 230°C and under a load of 2.16 kg) was used. All other chemicals including dicumyl peroxide (DCP, the initiator) and maleic anhydride (MAH, the reactive monomer) were of reagent grade and were used without further purification.

Melt mixing

The composition of the reaction mixture was typically 42 g PP, 0 to 10 phr MAH and 0 to 2 phr DCP. The components were mixed in a Haake-Buchler Rheomix 600 internal mixer (equipped with a pair of high-shear rollers) connected to the Rheocord 40 main frame. The temperature of the mixing chamber was set at 180°C. Half of the PP loading was first introduced into the mixing chamber and premelted at a rotor rate of 10 rpm for 1 min. At the end of the first minute, MAH was added and mixed at a rotor rate of 20 rpm for another period of 1 min. The remaining half of the PP loading and DCP were introduced into the mixing chamber at the end of the second minute and the rotor rate was increased to and maintained at 40 rpm thereafter. The total mixing time was 20 min. The final melt temperature (as measured by a thermocouple) lay consistently in the range of 180–185°C. The mixing torque was recorded throughout the entire mixing process. For a given composition, the reproducibility in the final torque value was within 0.5 N m.

Fourier-transform infra-red spectroscopy (FT*i.r.*)

The reaction products were pressed at ca. 180°C into thin films, from which i.r. spectra were taken using a Digilab FTS-40 *FT*i.r. spectrometer with the coaddition of 64 scans at a resolution of 2 cm^{-1}.

Dynamic rheological analysis

Dynamic rheological properties including storage modulus (G') and loss modulus (G'') of the reaction products were measured using the parallel-plate fixture in a Rheometrics RDA-II instrument in the frequency range of 1 to 400 rad s^{-1} at 185°C. The maximum strain was 10%, within the linear viscoelasticity range of the samples.

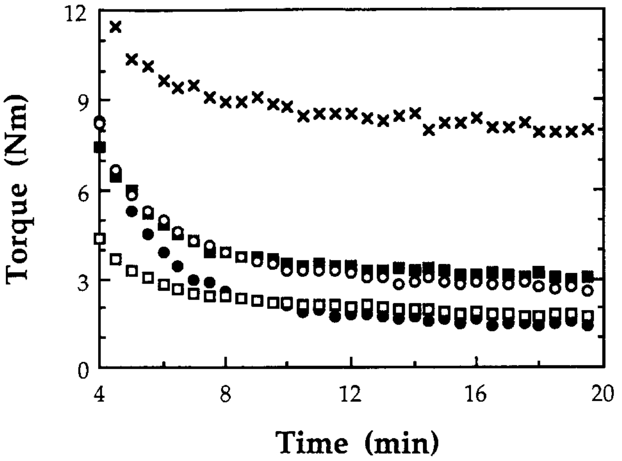

Figure 1 Representative torque curves of the reaction mixtures: (×), PP blank; (■), PP with the addition of 0.1 phr DCP only; (□), PP with the addition of 0.1 phr DCP and 0.2 phr MAH; (●), PP with the addition of 0.1 phr DCP and 0.5 phr MAH; (○), PP with the addition of 0.1 phr DCP and 2 phr MAH

Table 1 Mixing torque behaviour and dynamic rheological properties of the reaction products. The numbers in parentheses are estimated via extrapolation of experimental G' and G'' curves

DCP (phr)	MAH (phr)	Final torque[a] (N m)	G_x (kPa)	ω_x (rad s^{-1})
0	0	8.3	29	16
0	10	7.3	–	–
0.1	0	2.8	43	250
0.1	0.2	2.0	49	400
0.1	0.5	1.8	(42)	(580)
0.1	1	1.9	49	400
0.1	2	2.6	44	250
0.1	5	3.3	28	100
0.1	10	3.7	–	–
0.25	0	1.1	–	–
0.25	0.2	1.1	–	–
0.25	0.5	0.9	–	–
0.25	1	0.6	–	–
0.25	2	1.5	–	–
0.25	5	2.5	40	160
0.5	0	0.9	–	–
0.5	0.2	0.5	–	–
0.5	0.5	0.7	–	–
0.5	2	1.2	–	–
0.5	5	3.1	32	80
0.5	10	4.0	33	50
0.5	20	4.5	25	20
2.0	0	0.5	–	–
2.0	2	0.5	–	–
2.0	5	2.2	26	200
2.0	10	2.6	25	100
2.0	20	3.4	23	32

[a] Typically the average value from two or three runs

RESULTS

Mixing torque

Figure 1 shows typical torque curves for the present reaction systems. The characteristics of these torque curves include an early sharp peak due to material loading, followed by a plateau region of nearly constant mixing torque. For the sake of clarity, only the part of the torque curves beyond the loading peak (i.e. after 4 min of melt mixing) are presented. The final torque values (as given in *Table 1*) are used to rank qualitatively the viscosity level of the reaction products[17–19].

With DCP as the sole additive, the final torque values are clearly lower than that (i.e. ca. 8.3 N m) of the PP blank, suggesting the dominance of peroxide-initiated chain scission. It may be noted that this degradation effect is quite efficient with the first addition (i.e. 0.1 phr) of DCP, resulting in a two-thirds decrease (to ca. 2.8 N m) in the final torque. As the DCP content is increased slightly to 0.25 phr, the final torque is decreased to a

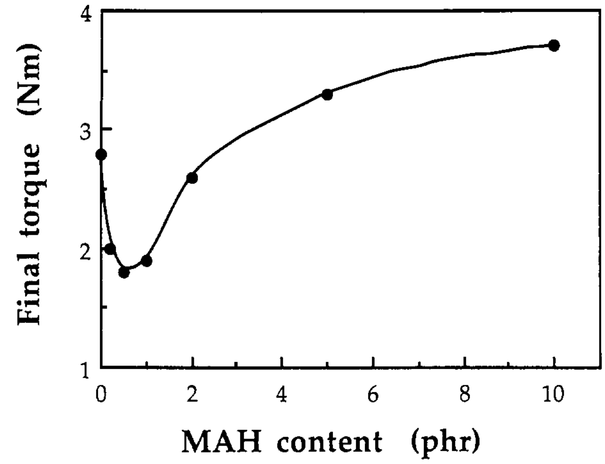

Figure 2 Variation of the final torque value with MAH loading at a fixed DCP level of 0.1 phr

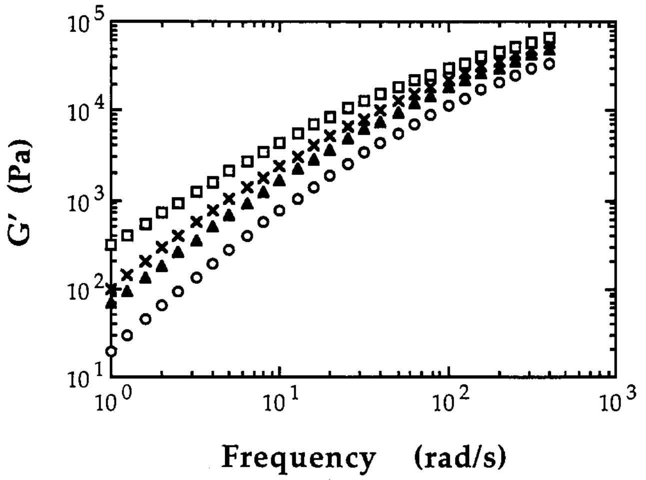

Figure 3 Variation of storage modulus with angular frequency at 185°C for the reaction products obtained at a fixed DCP loading of 0.1 phr: (×), without added MAH; (○), with 0.5 phr MAH; (▲), with 1 phr MAH; (□), with 5 phr MAH

dramatically low value of ca. 1.1 N m, only a small fraction of that for the PP blank. More interestingly, in the presence of MAH and with the DCP loading fixed, the final torque first decreases but then increases with the MAH loading (cf. *Figure 2* and *Table 1*), suggesting enhanced chain scission at low MAH levels but alleviated PP degradation at higher MAH levels.

Dynamic rheological analysis

Figure 3 gives representative G' vs. ω curves for reaction products of varying MAH loadings but at a fixed DCP level. The G' curves move downwards first but then upwards with increasing MAH content, showing the same trend as the final torque. Although not shown here, a similar behaviour is observed for the corresponding G'' vs. ω curves.

It has been shown[20,21] that the cross-over point of G' and G'' curves (i.e. $G' = G'' = G_x$ at $\omega = \omega_x$, cf. *Figure 4*) may be related to molecular parameters according to:

$$G_x \sim (M_w/M_n)^a \qquad (1)$$

and

$$\omega_x \sim (M_w)^b \qquad (2)$$

where M_w and M_n are weight- and number-average molecular weights, respectively, while a and b are *negative* exponents. The fact that ω_x decreases first and then increases with MAH loading (cf. *Figure 5* and *Table 1*) is also in good agreement with the suggested enhancement of chain scission at low MAH levels but alleviation of PP degradation at higher MAH loadings. It should be noted that the enhanced degradation at low MAH loadings is more prominent when the peroxide level is low. The variation of G_x with reaction composition is less pronounced but suggests a tendency for lower polydispersity upon chain scission. This is in agreement with previous observations[22,23] in controlled PP degradation.

Fourier-transform infra-red spectroscopy

Figure 6 shows represenstative *FT*i.r. spectra of the melt-processed materials. Important features include characteristic absorptions of the PP backbone rocking near 810 cm^{-1} and characteristic MAH carbonyl stretching bands at 1780 and 1860 cm^{-1}. With the addition of MAH alone, there appears no significant grafting of MAH onto PP; the anhydride bands are prominent only for the case of simultaneous addition of DCP and MAH. These observations indicate the lack of graft reaction when MAH was the only additive as well

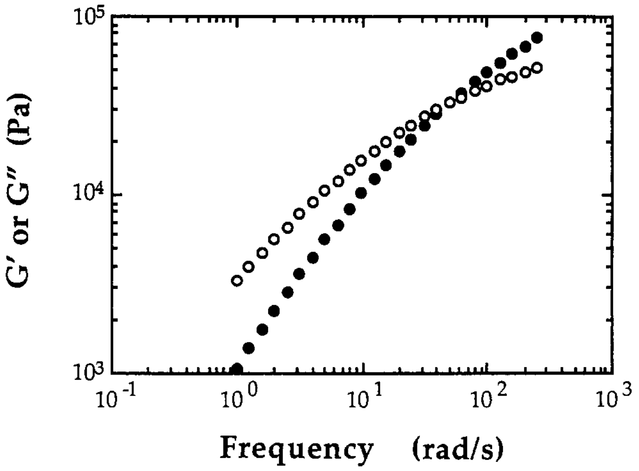

Figure 4 Cross-over of G' (●) and G'' (○) curves. This sample was obtained at DCP and MAH loadings of 0.5 and 10 phr, respectively

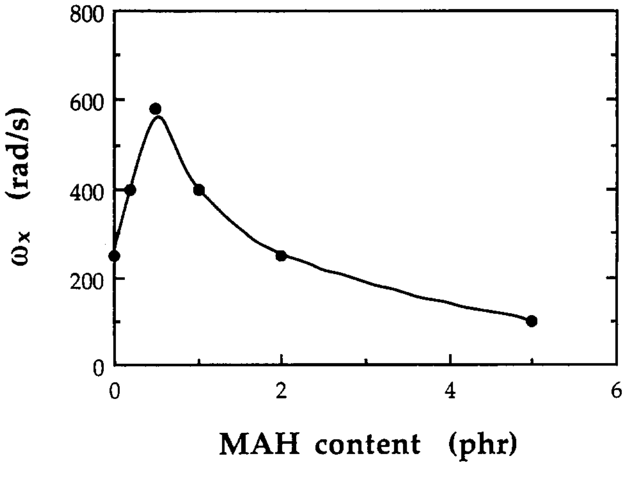

Figure 5 Variation of cross-over frequency (ω_x) with MAH loading at a fixed DCP level of 0.1 phr

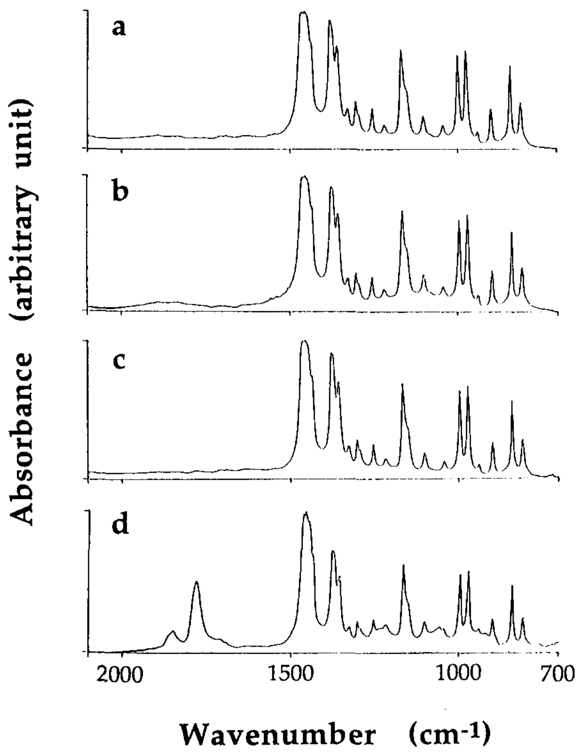

Figure 6 Representative *FT*i.r. spectra: (a) PP blank; (b) PP with the addition of 0.5 phr DCP only; (c) PP with the addition of 10 phr MAH only; (d) PP with the addition of 0.5 phr DCP and 10 phr MAH

Table 2 Efficiency of grafting

DCP (phr)	MAH (phr)	Relative peak height[a] at 1780 cm^{-1}	η_{DCP} (phr^{-1})	η_{MAH} (phr^{-1})	η (phr^{-1})
0.1	0.2	0.16±0.03	1.60	0.80	1.1
0.1	0.5	0.53±0.05	5.30	1.06	2.4
0.1	1	0.78±0.07	7.80	0.78	2.5
0.1	2	0.97±0.03	9.70	0.49	2.2
0.25	0.2	0.25±0.01	1.00	1.25	1.1
0.25	0.5	0.54±0.03	2.16	1.08	1.5
0.25	2	1.07±0.06	4.28	0.54	1.5
0.5	2	1.70±0.10	3.40	0.85	1.7
0.5	5	1.87±0.13	3.74	0.37	1.2
0.5	10	1.97±0.16	3.94	0.20	0.9
2.0	2	2.14±0.18	1.07	1.07	1.1
2.0	5	2.72±0.19	1.36	0.54	0.9
2.0	10	3.26±0.17	1.63	0.33	0.7

[a] Error bounds correspond to the 95% confidence limit

as the loss of MAH through evaporation during the rather long period of melt mixing. The boiling point of MAH is 202°C, only some 20°C above the processing temperature.

The extent of anhydride grafting is estimated as the ratio between height of the 1780 cm^{-1} band and that of the 810 cm^{-1} band. It may be observed from *Table 2* that the extent of grafting increases with increasing DCP and MAH contents, but the effects levels off at higher loadings of the additives. The effectiveness of the reactive additives may be accessed by use of the following definitions for efficiencies of the reactive ingredients:

$$\eta_{DCP} = \text{DCP efficiency factor} = (\text{relative peak height at } 1780\,cm^{-1})/(\text{DCP content}) \quad (3)$$

$$\eta_{MAH} = \text{MAH efficiency factor} = (\text{relative peak height at } 1780\,cm^{-1})/(\text{MAH content}) \quad (4)$$

$$\eta = \text{combined efficiency factor} = (\eta_{DCP}\eta_{MAH})^{0.5} \quad (5)$$

It is clearly demonstrated in *Table 2* that η_{DCP} increases with the MAH level but decreases with the DCP loading. Similarly, η_{MAH} increases with the DCP level but decreases with the MAH loading. The combined efficiency factor η, which represents the general effectiveness of the reactive ingredients, is at its maximum range when the DCP level is low (i.e. 0.1 phr in the present case) but the MAH level is comparatively high (in terms of the MAH/DCP ratio). This may be attributed to the low solubility of MAH in PP and the extensive peroxide-induced side reactions (as discussed in the following sections) involved.

DISCUSSION

The enhancement of PP degradation upon the addition of MAH, previously observed by Gaylord and Mishra[4], is confirmed in the present study. However, the scission of PP chains becomes less pronounced at higher MAH levels, similar to our previous observations[13]. The fact that the MAH-enhanced chain scission is more significant at low DCP and MAH levels serves to explain the stronger tendency towards chain scission (even for a rather high MAH loading of 5 phr at a DCP loading of 1 phr) in the experiment of Gaylord and Mishra: they added the MAH/DCP mixture portion-by-portion (four portions in total), therefore keeping DCP and MAH concentrations reasonably low but without depletion throughout the entire melt mixing process. It also explains why other studies[13,16] failed to recognize this phenomenon: the range of the enhanced degradation is observable only for a narrow range of MAH loading if the ingredients are loaded all at once. The basic mechanism of the MAH-enhanced degradation, however, remains to be clarified.

At this juncture, a closer look at the peroxide-initiated degradation itself is in order. The mechanism of peroxide-initiated PP degradation is often considered to include[4,22–25] (a) peroxide decomposition to form primary radicals, (b) hydrogen abstraction of a primary radical from a PP chain to form a tertiary (macro)radical, (c) chain breakage via β scission of the tertiary radical to generate a secondary radical, and (d) termination via either combination or disproportionation. This mechanistic scheme, however, is not completely satisfactory. The ratio of reactivities for the abstraction of tertiary and secondary hydrogens has been estimated as 6:1 by Loan[26] in his study of peroxide crosslinking of EPR. If the relative population of tertiary and secondary hydrogens in PP is considered, the ratio of the formation rates of tertiary and secondary radicals should be ca. 3:1, rendering the neglect of secondary radicals unjustified. In addition, earlier reports[26–28] of peroxide-induced crosslinking of PE and EPR indicated that both combination and disproportionation contributed significantly to the termination of secondary radicals.

Based on the considerations above, the following mechanistic scheme is proposed:

Initiator decomposition

$$I \rightarrow 2R^* \tag{6}$$

Hydrogen abstraction

$$-CH_2-CH(CH_3)- + R^* \rightarrow -CH_2-C^*(CH_3)-\ (^3P^*) + RH \tag{7}$$

$$-CH_2-CH(CH_3)- + R^* \rightarrow -C^*H-CH(CH_3)-\ (^2P^*_c) + RH \tag{8}$$

β scission

$$-CH_2-C^*(CH_3)-CH_2-CH(CH_3)-\ (^3P^*) \rightarrow C^*H(CH_3)-\ (^2P^*_t) + -CH_2-C(CH_3){=}CH_2 \tag{9}$$

Chain transfer

$$-CH_2-CH(CH_3)- + C^*H(CH_3)-\ (^2P^*_t) \rightarrow -CH_2-C^*(CH_3)-\ (^3P^*) + -CH_2- \tag{10}$$

$$-CH_2-CH(CH_3)- + -C^*H-\ (^2P^*_c) \rightarrow -CH_2-C^*(CH_3)-\ (^3P^*) + -CH_2- \tag{11}$$

Termination via combination

$$2\,^2P^*_c \rightarrow P-P \text{ (crosslinking)} \tag{12}$$

$$2P^*_c + {}^2P^*_t \rightarrow P-P \text{ (branching)} \tag{13}$$

$$2P^*_c + {}^3P^* \rightarrow P-P \text{ (crosslinking)} \tag{14}$$

Termination via disproportionation

$$2\,^2P^*_c \rightarrow 2P \tag{15}$$

$$^2P^*_c + {}^2P^*_t \rightarrow 2P \tag{16}$$

$$^2P^*_c + {}^3P^* \rightarrow 2P \tag{17}$$

$$^2P^*_t + {}^3P^* \rightarrow 2P \tag{18}$$

$$2\,^3P^* \rightarrow 2P \tag{19}$$

Here, $^3P^*$ and $^2P^*_c$ represent respectively the tertiary and the ('central') secondary radicals from hydrogen abstraction, $^2P^*_t$ represents the ('terminal') secondary radical from β scission of $^3P^*$, and P and P–P represent the dead (linear, branched, or crosslinked) polymers. Considering the number of available α-hydrogen atoms as well as the steric effect[29], we have assumed that combination reactions (i.e. equations (12)–(14)) involve mainly $^2P^*_c$ radicals.

In the case of low peroxide concentrations, termination reactions are rare owing to low radical concentrations. Hence, the chain transfer/β scission reaction route (i.e. equations (9) and (10)) dominates; the cyclic nature of equations (9) and (10) renders the peroxide-initiated PP degradation process highly efficient. In the case of high peroxide levels, crosslinking via biomolecular coupling becomes important. These features are consistent with previous observations of peroxide-induced degradation or crosslinking of PP.

In the presence of MAH, additional reactions occur. They probably include the following:

Anhydride grafting

$$^3P^* + C_4H_2O_3\ (M) \rightarrow -C(CH_3)(C_4H_2O_3)^*-\ (PM^*) \tag{20}$$

$$^2P^*_c + C_4H_2O_3\ (M) \rightarrow -CH(C_4H_2O_3)^*-\ (PM^*) \tag{21}$$

$$^2P^*_t + C_4H_2O_3\ (M) \rightarrow (CH_3)CH(C_4H_2O_3)^*-CH_2-\ (PM^*) \tag{22}$$

Chain transfer

$$-CH(CH_3)- + PM^* \rightarrow {}^3P^* + PM \tag{23}$$

Termination via combination

$$PM^* + {}^2P^*_c \rightarrow PM-P \text{ (crosslinking or branching)} \tag{24}$$

Termination via disproportionation

$$2PM^* \rightarrow 2PM \tag{25}$$

$$PM^* + {}^2P^*_t \rightarrow 2PM + P \tag{26}$$

$$PM^* + {}^3P^* \rightarrow 2PM + P \tag{27}$$

Here, M, PM* and PM represent MAH, the secondary radical after anhydride grafting and the corresponding dead polymer, respectively. It is assumed that the secondary PM* radical is less reactive (as compared to other secondary radicals) by considering the steric effect as well as the electronic stabilization due to the neighbouring carbonyl group. Note that the chain transfer steps (i.e. equation (14)) can be *intra*molecular (as proposed by Greco *et al.*[6] for grafting of dibutyl maleate onto EPR) or *inter*molecular reactions. The presence of various sites (single-ring appendage, chain-end attachment and crosslinking points) here reflects our belief that the previously observed sites are all possible; the corresponding reaction paths compete with one another. Differences in experimental conditions render the predominance of different sites in previous studies.

At low peroxide and MAH concentrations, PM* radicals lack the opportunity of bimolecular coupling and tend to undergo chain transfer (equation (23)), yielding tertiary radicals undergoing the β scission/$^3P^*$ regeneration cycle (equations (9) and (10)). In this case, the presence of MAH serves to lower the concentration of the combination-prone $^2P^*_c$ radicals, resulting in enhanced PP degradation. As the MAH concentration increases, bimolecular coupling reactions (equation (24)) become more significant owing to the increased population of PM* from equations (20)–(22). The competition between bimolecular coupling (equation (24)) and chain transfer/β scission (equations (23), (9) and (10)) therefore results in the alleviation of PP degradation.

CONCLUSIONS

Functionalized PP, prepared by melt mixing with various amounts of DCP and MAH, has been analysed by means of dynamic rheological analysis and Fourier-transform infra-red spectroscopy. With the addition of MAH alone, there appears no discernible grafting of MAH onto PP. Grafting of MAH may be realized only with the simultaneous presence of DCP and MAH. The optimal composition for the present reaction system appears to be at a low DCP level and a moderate MAH loading.

With DCP as the sole additive, PP exhibits significant degradation during processing. The scission of PP chains becomes more extensive on the first addition of MAH. Upon further increase in the MAH level, however, the trend is reversed and the degradation of PP appears alleviated. This is explained in terms of the competition between chain transfer/β scission and combination reactions.

REFERENCES

1 Paul, D. R. in 'Polymer Blends' (Eds. D. R. Paul and S. Newman), Academic Press, New York, 1978, Ch. 12

2 Gaylord, N. G. *Chemtech* 1989, **19**, 435

3 Gaylord, N. G. and Mehta, M. *J. Polym. Sci., Polym. Lett. Edn.* 1982, **20**, 481

4 Gaylord, N. G. and Mishra, M. K. *J. Polym. Sci., Polym. Lett. Edn.* 1983, **21**, 23

5 Gaylor, N. G., Mehta, M. and Mehta, R. *J. Appl. Polym. Sci.* 1987, **33**, 2549

6 Greco, R., Maglio, G. and Musto, P. V. *J. Appl. Polym. Sci.* 1987, **33**, 2513

7 Wu, C. H. and Su, A. C. *Polym. Eng. Sci.* 1991, **31**, 1629

8 Wu, C. H. and Su, A. C. *Polymer* 1992, **33**, 1987

9 Minoura, Y., Ueda, M., Mizunuma, S. and Oba, M. *J. Appl. Polym. Sci.* 1969, **13**, 1625

10 Russell, K. E. and Kelusky, E. C. *J. Polym. Sci., Polym. Chem. Edn.* 1988, **26**, 2273

11 Rengarajan, R., Parameswaran, V. R., Lee, S., Vicic, M. and Renaldi, P. L. *Polymer* 1990, **31**, 1703

12 Constable, R. C. and Adur, A. M. Proceedings of the 49th Annual Technical Conference, Soc. Plast. Eng., Montreal, 1991, p. 1892

13 Wu, C. H., Su, A. C. and Chen, S. I. Proceedings of the 12th ROC Polymer Symposium, Hsinchu, Taiwan, 1988, p. 332

14 Kunert, K. A., Ranachowski, J., Chodak, I., Soszynska, H. and Pislewski, N. *Polymer* 1981, **22**, 1677

15 Chodak, I. and Lazar, M. *J. Appl. Polym. Sci.* 1986, **32**, 5431

16 Hogt, A. H. Proceedings of the 2nd International Congress on Compatibilizers and Reactive Polymer Alloying, New Orleans, 1990, p. 179

17 Goodrich, J. E. and Porter, R. S. *Polym. Eng. Sci.* 1967, **7**, 45

18 Blyer, L. L. Jr and Daane, J. D. *Polym. Eng. Sci.* 1967, **7**, 178

19 Lee, G. C. N. and Purdon, J. R. *Polym. Eng. Sci.* 199, **9**, 360

20 Utracki, L. A. and Schlund, B. *Polym. Eng. Sci.* 1987, **27**, 367

21 Utracki, L. A. in 'Multiphase Polymers: Blends and Ionomers' (Eds. L. A. Utracki and R. A. Weiss), American Chemical Society, Washington, DC, 1989, Ch. 7

22 Suwanda, D., Lew, R. and Balke, S. T. *J. Appl. Polym. Sci.* 1988, **35**, 1033

23 Tzoganakis, C., Vlachopoulos, J. and Hemielec, A. E. *Polym. Eng. Sci.* 1988, **28**, 170

24 Borsig, E., Fiedlerova, A. and Lazar, M. *J. Macromol. Sci.–Chem.* (*A*) 1981, **16**, 513

25 Chodak, I. and Zimanyova, E. *Eur. Polym. J.* 1984, **20**, 81

26 Loan, L. D. *J. Polym. Sci.* (*A*) 1964, **2**, 3053

27 van Drumpt, J. D. and Oosterwijk, H. H. J. *J. Polym. Sci., Polym. Chem. Edn.* 1976, **14**, 1495

28 Hulse, G. E., Kersting, R. J. and Warfel, D. R. *J. Polym. Sci., Polym. Chem. Edn.* 1981, **19**, 655

29 Lenz, R. W. 'Organic Chemistry of Synthetic High Polymers', Interscience, New York, 1971, p. 354